

On The Design of a Hydraulically Actuated Finger For Dextrous Manipulation

Daniel F. Schmidt, Gordon S. Lowe, Andrew P. Paplinski

Department of Computer Science and Software Engineering

Monash University

Melbourne, Australia

Email: {Daniel.Schmidt, Gordon.Lowe, Andrew.Paplinski}@csse.monash.edu.au

Abstract— We propose an actuator for multi-fingered grippers for industrial robots built around fluid-powered bladders enclosed within the structure of the phalanges themselves. Unlike a normal hydraulic cylinder where the available force is a function of the height and width of the phalanges, in this configuration, the force the fingers can generate becomes a function of the length and width of the phalange. The proposed design is mechanically simple with all actuation elements contained within the phalanges themselves, and has minimal moving parts. This paper presents the dynamic and static characteristics of a finger built from three of these actuators, and simulation results show that the fingertip forces the proposed fingers can generate make them suitable for application in an industrial environment.

I. INTRODUCTION

Artificial and robotic hands, for both industrial and prosthetic use, have been an active field of research for at least the last twenty years. During this period, one recurring issue has been the actuators used to supply power to the fingers of the hands. An ideal actuator must be able to deliver high finger forces while remaining compact, mechanically simple and relatively inexpensive. This paper presents research on a hydraulically powered actuator design for fingers that goes somewhat towards realising these requirements.

II. PREVIOUS WORK

Work on artificial hands that can perform grasping of objects, as well as manipulation, has been ongoing since the early 1980s. It can be roughly divided into two basic areas: prosthetic hands designed to replace human hands for medical purposes, and hands that are to be fitted to industrial robots in an attempt to extend the flexibility of robot systems.

Early studies of grasping were done by Salisbury and Mason [7], and this work was focused on analysing hand designs and the grasps obtainable by various designs. From this work it was determined that a hand with three fingers, each with three DOF, would be sufficient to provide stable grasps capable of force closure on arbitrary objects. This work directly led to the design of the Stanford/JPL hand [7], a three fingered hand powered by electric motors. The motors transferred power to the fingers through Teflon coated, flexible cables, which while reducing the mass of the hand itself introduced complexity in the drive mechanism and required accurate sensing of the cable tensions to allow for good control.

Since this earlier work a large range of hands have been designed. The groundbreaking MIT/Utah [5] hand was a pneumatically powered, four fingered, tendon based hand that, while possessing many degrees of freedom, was complex and very expensive. Electric motors have also proved to be popular power sources for hands, with recent designs still employing them as the primary power source [1]. The Goldfinger [9] hand is a four-fingered hand, this time with the fingers arranged in an alternate ‘raptor’ like fashion, which uses electric motors and a complex linkage system to transmit power to the fingers. The Robonaut [6] hand is a five fingered design made to mimic the human hand and also uses electric motors to actuate the fingers, though in this case tendons are avoided by the use of special leadscrew/flex shaft assemblies that are used convert the rotary motion to linear motion. While all of these hands perform well they are all very mechanically complex, and the forces they can produce are limited by the power of the electric motors they use.

There have been a variety of hydraulic hand designs. Most of these use conventional hydraulic cylinders to actuate the fingers, often transmitting power through a linkage system [4]. A lightweight prosthetic hand developed recently by the Karlsruhe Institute of Applied Computer Science [10] uses flexible fluidic actuators that are based around inflatable diaphragms that are placed between each phalange. This hand is specifically designed to replace human hands and as such its force capabilities are low but it demonstrates that integration of simple hydraulic actuators similar to the ones we propose into the hand itself can lead to a compact and simple solution.

Control of fluid power systems, especially if the volume of fluid is small and the operating pressures high, is a significantly more complex than control of electric motors. Recent work by Sohl and Bobrow [11] has demonstrated excellent force and position tracking of a small volume hydraulic cylinder, running at high pressure - similar in nature to the proposed actuator. Traditionally, pneumatic power - despite enjoying several advantages over hydraulic power - has been appropriate only for tasks requiring movement between fixed endpoints. However, recent research has shown that with the increase in power of microcomputers it is possible to improve the performance of pneumatic servo control through the use of advanced controllers that account for the compressibility of air [2]. Both works suggest that fluid power, despite the

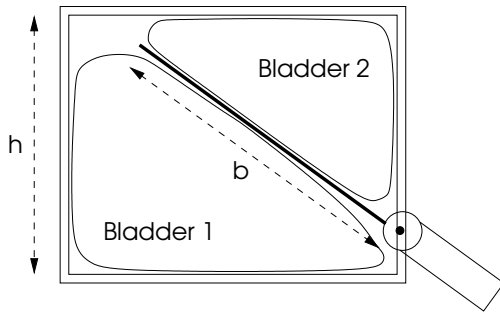


Fig. 1. Actuator Configuration 1

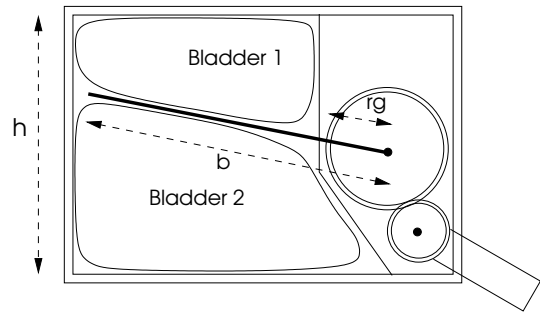


Fig. 2. Actuator Configuration 2

compressibility issues, is a suitable choice for actuation of fingers where good stiffness control is required.

Previously, a single phalange prototype finger based around actuation by an enclosed bladder has been constructed and its static performance tested [3]. In this paper we extend the work to include a dynamic model of the actuator including the effects of the fluid compressibility, propose a complete finger based around these actuators, and evaluate its expected static and dynamic performance through simulation.

III. ACTUATOR CONFIGURATIONS

There are two basic configurations for the actuators.

A. Configuration 1: Cantilevered Beam

In this configuration the bladder directly actuates the beam that is attached to a rotary joint (Figure 1). This configuration provides direct rotary motion of the next phalange without requiring any gearing or linkages, and thus avoids backlash and has low static friction characteristics. However, for a fully enclosed phalange, if the height is less than the length the actuator will not be able to travel through ninety degrees. If θ is the angle between the beam and the bottom of the phalange structure in Figure 1, given a beam length b and phalange height h , the maximum angle the beam can attain is given by

$$\theta_{\max} = \sin^{-1} \left(\frac{h}{b} \right) \quad (1)$$

Clearly, if $b = h$ then the phalange will have a full ninety degree travel, but will become bulkier.

B. Configuration 2: Geared Actuator

In this configuration the rotary motion from the beam is geared up to provide a bigger range of travel, at the expense of some torque (see Figure 2). The maximum angle of beam travel, $\theta_{B\max}$, is the angle between the most positive and most negative deflections the beam can attain w.r.t. the bottom of the phalange. The gearing ratio, N , that will allow for ninety degrees of actuator travel is given by

$$N = \frac{0.5\pi}{\theta_{B\max}} \quad (2)$$

Assume the beam angle, θ_B , is measured from the most positive beam deflection, and increases in a counter-clockwise direction. If θ_A is the angle of the actuator link, then

$$\theta_A = N\theta_B \quad (3)$$

IV. ACTUATOR DYNAMICS

The considered actuator utilises hydraulic fluid power by inflating a bladder like arrangement that effectively provides a seal for the fluid. The developed dynamics model takes into account compressibility of the fluid because the operating pressures will be high and the fluid mass will be small, i.e. conditions which begin to violate the incompressible liquid approximation.

A. Bladder Dynamics

From the flow continuity equation [13], the basic dynamics of the bladder including the effects of fluid compressibility can be found as

$$q_i - q_o = \dot{V} + \frac{V}{\beta} \dot{p} \quad (4)$$

where V is the volume, β is the bulk modulus, p is the pressure and q_i and q_o are the flow in and out of the bladder. For a bladder with a single connection, q_o is always zero and q_i is either positive (for flow in) or negative (for flow out). Rearranging (4) gives the differential equation

$$\dot{p} = \frac{\beta}{V} (-\dot{V} + q) \quad (5)$$

where q is now flow into or out of the bladder. The total system bulk modulus will include the bulk modulus of both the fluid and the bladder material. The volume of the bladder for a given beam angle, θ , is determined by its geometric shape. The bladder will be deformable and its volume and the area of contact between it and the beam will vary depending on the force being exerted by it, but modeling this is currently difficult due to the very nonstandard nature of the bladder. Consequently, the simple approximation that the bladder will entirely fill the region beneath/above the beam and will maintain full contact against the beam at all times is assumed. A more complete model will be experimentally determined after a study on possible bladders has determined an appropriate shape and material. Given this assumption, the volumes of the bladders can be found from simple geometry, and the area of contact between the bladder and the beam will be given by

$$A = bw \quad (6)$$

where b is the length of the beam, and w is the width of the beam.

B. Servo Valve Dynamics

The servo valve is used to direct fluid flow into or out of the bladders. The most accurate servo valve dynamic models are high order and nonlinear in nature, and require measurement of the spool position. As the time constants involved in these higher order models are much lower than the hydraulic time constants, a first order nonlinear approximation has been used instead. The spool position, s , is given by:

$$t_s \dot{s} = -s + u \quad (7)$$

where u is the input current command, and t_s is the equivalent time constant of the servo valve. A five-port servo valve is used, connected up as in [11]. The spool position is given by (7), and there are two flows, q_1 and q_2 , to bladders 1 and 2 respectively. These are given by

$$q_1 = \begin{cases} c_1 s \sqrt{p_s - p_1} & \text{for } s \geq 0 \\ c_2 s \sqrt{p_1 - p_r} & \text{for } s < 0 \end{cases} \quad (8)$$

and

$$q_2 = \begin{cases} -c_3 s \sqrt{p_2 - p_r} & \text{for } s \geq 0 \\ -c_4 s \sqrt{p_s - p_2} & \text{for } s < 0 \end{cases} \quad (9)$$

where c_1, \dots, c_4 are valve flow coefficients, p_1 and p_2 are the pressures in the two bladders, and p_s and p_r are the supply and reservoir pressures (above atmospheric pressure).

C. Double Acting Actuator Configuration 1

A double acting actuator built from two bladders in the configuration described in section III-A (see Figure 1) is able to exert similar force in both an inwards grasping direction and in the release direction. Finger contacts are unisense in nature, and for grasping tasks high release forces are not required and thus a single acting configuration with a spring for return could be employed. However, a double acting configuration ensures release and grasp speeds and forces are similar. This increases the functionality of the hand, allowing it to manipulate objects by pushing with the back of the fingers. Taking the derivative of the force exerted on the beam by both bladders gives:

$$\dot{F} = A(\dot{p}_1 - \dot{p}_2) \quad (10)$$

where A is given by (6). The torque developed on the beam due to the force exerted on it by the bladder can be found if it is treated as a simply supported beam with a distributed load. The fraction along the beam, x_F , at which the equivalent single force acts is given by

$$x_F = \frac{0.5(b + c_x)}{b} \quad (11)$$

where c_x is the distance from the pivot to the bladder. In this configuration, c_x will usually be zero. The total torque developed on the beam also includes frictional torques and the inertial torque of the beam (and attached link)

$$I\ddot{\theta} = x_F b F - h(\dot{\theta}) - \tau_L \quad (12)$$

where $h(\dot{\theta})$ are frictional torques, I is the moment of inertia of the beam and link, b is the length of the beam, and τ_L is torque introduced by a grasped load.

D. Double Acting Actuator Configuration 2

For a double acting phalange in configuration 2 (see Figure 2), the torque developed on the finger mass is given by

$$I_L \ddot{\theta}_A = \tau_A - h_A(\dot{\theta}_A) - \tau_L \quad (13)$$

where I_L is the moment of inertia of the finger link, τ_L is torque introduced by a grasped load and $h_A(\dot{\theta}_A)$ are frictional torques. The torque from the gear pair is proportional to the torque on the beam, τ_B , by

$$\tau_A = N\tau_B \quad (14)$$

where N is defined by (2). Due to the requirement of a gear in this configuration, the bladder will not act along the whole length of the beam. In this case, in (11), $c_x \approx r_g$, where r_g is the radius of the gear. This value will vary as the beam rotates, but with suitable design the variation can be made sufficiently small as to be negligible. The torque developed by the beam includes torques due to the force exerted on the beam by the bladder, frictional torques and the inertial torque of the beam and attached gear

$$\tau_B = x_F b F - h_B(\dot{\theta}_B) - I_B \ddot{\theta}_B \quad (15)$$

where $h_B(\dot{\theta}_B)$ are frictional torques, I_B is the moment of inertia of the beam and gear, and (10) describes the force exerted on the beam by the bladder. Substituting (3), (14) and (15) into (13) yields

$$\left(I_L + \frac{1}{N^2} I_B \right) \ddot{\theta}_A = \frac{1}{N} x_F b F - h(\dot{\theta}_A) - \tau_L \quad (16)$$

where

$$h(\dot{\theta}_A) = h_A(\dot{\theta}_A) + \frac{1}{N} h_B\left(\frac{1}{N}\dot{\theta}_A\right) \quad (17)$$

is a combined function of the two frictional torques.

V. FINGER DESIGN

Given the models for individual phalanges, a full finger can be designed. Three phalanges give three DOF in the finger, and three fingers with three DOF allow for force closure when grasping arbitrary objects [7]. The proximal and distal phalanges will both use configuration 1 as it is simplest. For the proximal phalange, the extra height required can be accommodated as it will be contained within the palm, and in the case of the distal phalange, the overall length of the beam can be made small because it is the final link and the loading torques are the smallest. The intermediate phalange will use configuration 2 as it should be kept as thin as possible to allow the hand a greater range of functionality. All three phalanges are designed to have 90° range of motion. The design is shown in Figure 3. For the following discussion, it is assumed the finger is fully outstretched down the x -axis when $\theta_1 = \theta_2 = \theta_3 = 0^\circ$.

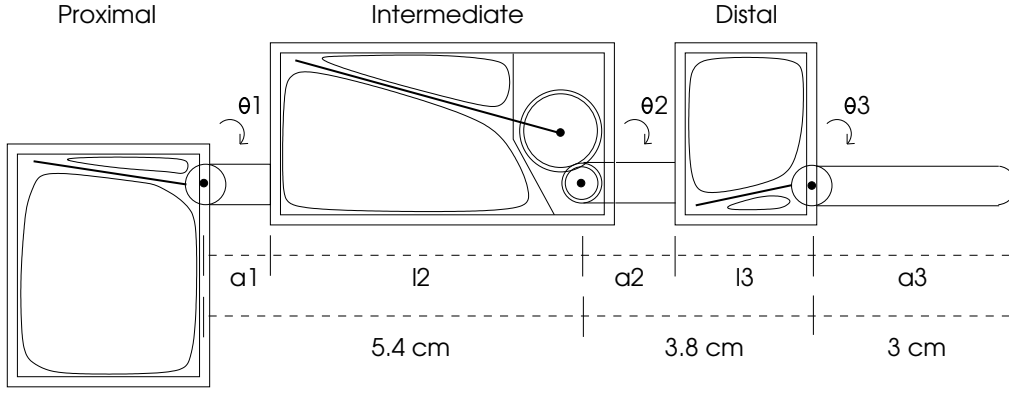


Fig. 3. Three Degree-of-Freedom Finger

A. Kinematics

No linkages are required to drive the fingers, so the forward kinematics for the three jointed finger are subsequently very simple, and are given by

$$x = (a_1 + l_2)c_1 + (a_2 + l_3)c_{12} + a_3c_{123} \quad (18)$$

$$z = (a_1 + l_2)s_1 + (a_2 + l_3)s_{12} + a_3s_{123} \quad (19)$$

where a_1, \dots, a_3 are the link lengths of the three phalanges, and l_1, \dots, l_3 are the lengths of the phalanx themselves. Inverse kinematics solutions for the joint angles $\theta_1, \dots, \theta_3$ are easily derived from these expressions.

B. Statics

1) *Force Exertion*: To find the static performance of the finger, it is modelled as a chain of links [8]. Given an external force, F_x , applied to the fingertip, the torque acting on link n is given by

$$\tau_{n-1,n} = \tau_{n,n+1} + \mathbf{p}_{n-1,n} \times \mathbf{f}_{n,n+1} + \mathbf{c}_{n-1,n} \times m_n \mathbf{g} \quad (20)$$

where $x_{n,n+1}$ is the variable x of link $n+1$ as seen by link n , expressed w.r.t. the base reference frame, $\mathbf{p}_{n-1,n}$ is the position of the end of the link, $\mathbf{c}_{n-1,n}$ is the centre of mass of the link, m_n is the mass of the link, $\mathbf{f}_{n,n+1}$ is the end-effector force, and \mathbf{g} is acceleration due to gravity. As each joint has only one degree of freedom, the only torque the actuators need to compensate for will be acting around the axis of rotation. This is found by

$$\tau_n = \tau_{n-1,n} \cdot \mathbf{z}_n \quad (21)$$

where \mathbf{z}_n is the unit vector describing the z -axis of the joint with respect to the reference frame. Evaluation for each joint, with a specified F_x , will yield the maximum torque the actuators must supply for static conditions. The static performance of an actuator can be found by taking $\dot{\theta}_n = \ddot{\theta}_n = \dot{p}_1 = \dot{p}_2 = p_2 = 0$

$$\tau_{\text{static}} = \frac{1}{N} x_F p b^2 w \quad (22)$$

where x_F is given by (11). From (22) it can be seen the maximum torque the actuator can produce is a function of the square of the length of the beam (and hence the phalanx).

This is advantageous as the loading torque given in (20) will only be a linear function of length of the attached link. Given a set of dimensions for the phalanges, (20), (21) can be evaluated for each joint and (22) solved to give the required operating pressure to meet the static torque requirements.

2) *Deflection Under Load*: Given the actuator uses a hydraulic power source it can resist greater forces than it can exert. If the control valve is closed, forces applied to the finger will result in the pressure in the bladder increasing until force equilibrium is achieved. From (5) and (10), with $q = 0$, we have

$$\dot{V} = -\frac{V\dot{\theta}}{\beta A} \quad (23)$$

and as V is a function of beam position θ the deflection under load can be determined. The maximum force the finger can resist is limited by the maximum forces the beam can withstand, and the maximum operating pressure of the bladder. It must be noted that although the finger can resist greater forces it loses control if the pressure increases above the standard operating pressure, and is thus only useful for grasping large loads if force closure can be achieved. It should also be noted that this deflection is purely for compression of the fluid and further deflection may occur due to bending of the finger structure itself.

C. Dynamics

Treating the finger as a serial-link manipulator [8], the torque developed on the links is given by

$$\tau = D(\theta)\ddot{\theta} + H(\theta, \dot{\theta}) + G(\theta) + \tau_e \quad (24)$$

where $D(\theta)$ is the inertia of the links, $H(\theta, \dot{\theta})$ are the Coriolis and centrifugal torques, $G(\theta)$ accounts for gravity and τ_e is the externally applied end-effector torque. The full equation of motion for the finger, including the actuator dynamics, is found by replacing the left hand side of either (12) (for configuration 1) or (16) (for configuration 2) (as $I_B \ll D(\theta)$) with the right hand side of (24), and dropping the τ_L term.

D. Sensing

The finger requires both force and position sensors. A strain gauge can be mounted to the beam to provide force

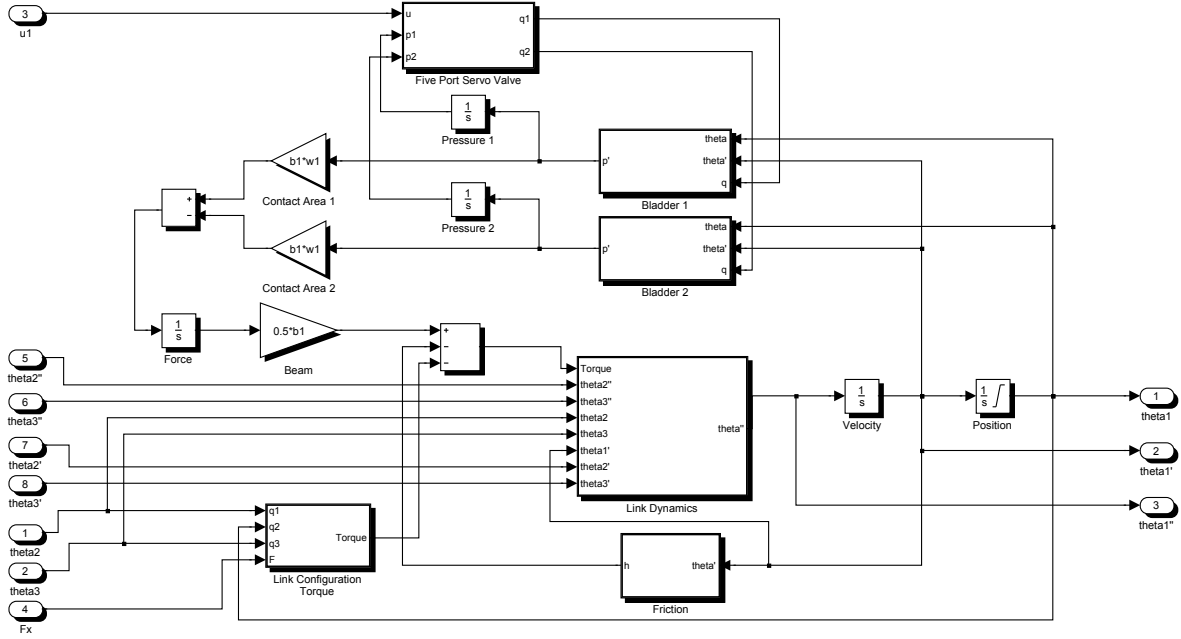


Fig. 4. Block Diagram of Actuator 1

measurement, and Hall effect sensors can be mounted on the finger to measure position.

VI. SIMULATION

Simulation of the complete finger was done in Matlab'sTM SimulinkTM package. Suitable physical parameters were selected and several simulation runs were used to determine the static performance and dynamic response of the full finger. Simulation of the finger was done by evaluating equations (5), (7), (8-9), (10), (12) for phalanges 1 and 3, (16) for phalange 2, and finally (24). Figure 4 shows the block diagram of a single actuator, the top half constituting the servo valve and bladder and the bottom half the dynamics, configuration dependent torque of the links and friction terms.

A. Simulation Parameters

A scale diagram of the full finger is shown in Figure 3. It is assumed the finger structures are made from aluminium and the gear pair is made of steel for extra strength. Given this, the centres of mass, the mass and the moments of inertia of each phalange were determined. A Moog 72 series servo valve was selected ($t_s \approx 0.02s$) and the system pressure was chosen as 1.379 MPa (200 PSI), with a typical hydraulic oil ($\rho = 825kg/m^3$, $\beta = 8.3 \times 10^8 N/m^2$) used as the fluid, and the control input $u \in [-1, 1]$.

B. Static Performance

The static performance of the finger can be assessed by evaluating (20) and (22) and determining the maximum F_x the finger can exert for varying finger configurations. The best-case static configuration is when $\theta_1 = \theta_3 = 0^\circ$ and $\theta_2 = 90^\circ$, with the finger operating with gravity in the $x-z$ plane and with the fingertip force exerted down the second and third

links. In this configuration, the expected force the finger can exert is approximately $193N$. The worst-case configuration is when $\theta_1 = \theta_2 = \theta_3 = 0^\circ$, with the finger operating in the $x-z$ plane against gravity with the fingertip force exerted against the fingertip up the z -axis. In this configuration the force the finger can exert is approximately $93N$. Even factoring in modelling errors, both of these values compare very well to other existing hand designs, including pneumatic designs (MIT/Utah, 30 N tip force [5]), electric motor designs (Barrett Hand, 20 N [12]) and other hydraulic hands (TUM hand, 30 N [4]). With a supply pressure of 685 KPa (if it was run pneumatically), the worst-case fingertip force is 42 N, which still compares well.

C. Dynamic Response

The dynamic response of the finger to both step and sinusoidal inputs was determined. To test the finger's step response, a smooth step input of the form $u = \tanh(50t)$ was applied at $t = 0s$, and a negative step of the same form applied at $t = 0.75s$, which tests both the closing and opening response time of the finger. With the friction term unknown, the tests have been performed to determine the maximum friction that still gives a reasonable closing time of $0.5s$. For a maximum frictional torque of $6 Nm$ for the proximal and intermediate phalange, and $4 Nm$ for the distal phalange, the response of each phalange is shown in Figure 5. The distal phalange has the slowest response, approximately $0.5s$, which is then the maximum closing time for a grasp. However, this will normally be lower, especially considering in the case of a human hand the relationship between proximal and intermediate phalange is usually $\theta_3 = 2\theta_2/3$. It can be confirmed that as the finger uses double acting actuators, the

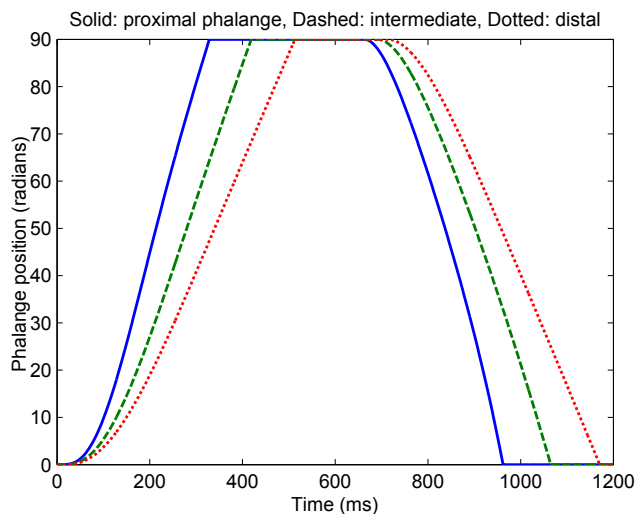


Fig. 5. Step responses of phalanges

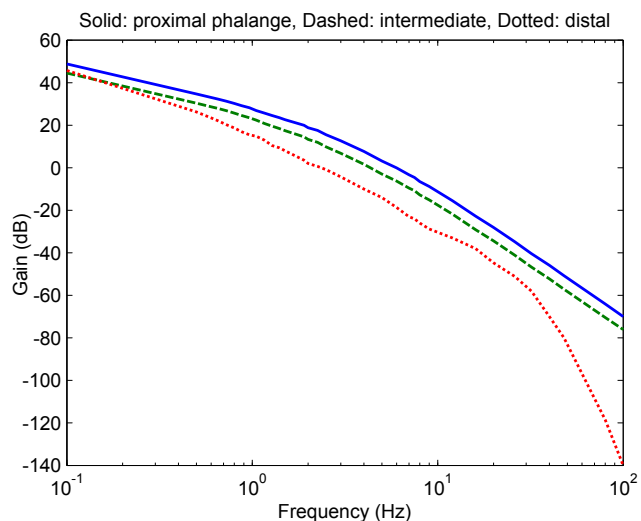


Fig. 6. Frequency responses of phalanges

closing and opening times are very similar.

The frequency response of the phalanges with the previously stated levels of friction is shown in Figure 6. The frequency response was found by applying a series of 0.02 peak-to-peak sinusoidal inputs to each phalange, with each phalange initially in the 45° position. It can be observed that the bandwidths of the phalanges are 7 Hz, 5 Hz and 3 Hz for the proximal, intermediate and distal phalanges respectively, all of which are reasonable for small movements of grasped objects. Although the system is nonlinear and this bandwidth is not universal for all finger configurations, it gives a good general indication of the dynamic performance of the finger. The step and frequency responses were both run with a supply pressure of 1.379 MPa.

Simulation results confirm that given the small mass and the low velocity of the finger, the variables with the greatest effect on the dynamic response are the friction and the flow rate into the bladders. The 'static' friction can be accounted for by nonlinear controllers assuming sufficient force is available. However, the results indicate that the prototype design must ensure that the friction while the fingers are moving is kept to a minimum.

VII. LIMITATIONS AND FUTURE WORK

Further work will involve procuring a suitable bladder and experimentally determining its expansion and friction characteristics. The internal shape of the actuators will subsequently be optimised to ensure maximum contact between beam and bladder, and to minimise friction. The complete stiffness of the finger in all configurations will be determined and suitable nonlinear controllers created for stiffness control. A prototype finger will be constructed, guided by these new presented results.

VIII. CONCLUSION

This paper presented a design for a three degree of freedom, hydraulically powered finger. This design delivers fingertip forces that compare very favourably to existing designs and

is mechanically extremely simple, requiring only four moving parts (two joints and a gear pair) and no complex linkages or tendons. It allows for easy integration of sensors and could conceivably be operated pneumatically and still provide reasonable fingertip forces. Simulation results show that with reasonable levels of friction, a closing time of 0.5s can be achieved, which is suitable for most industrial tasks.

REFERENCES

- [1] D. L. Arkin et al., "Development of a Four-Fingered Dexterous Robot End Effector For Space Operations", *Proceedings of the 2002 IEEE International Conference on Robotics and Automation*, pp. 2302-2308
- [2] J. E. Bobrow and B. W. McDonell, "Modeling, Identification, and Control of a Pneumatically Actuated, Force Controllable Robot", *IEEE Transactions on Robotics and Automation*, Vol. 14, No. 5, pp. 732-742, 1998
- [3] W. R. Doulis and G. S. Lowe, "Micro Actuator", *Proceedings of the 30th International Symposium on Robotics*, pp. 731-736, 1999
- [4] F. Pfeiffer, "Grasping with Hydraulic Fingers - An Example of Mechatronics", *IEEE/ASME Transactions on Mechatronics*, Vol. 1, No. 2, pp. 158-167, 1996
- [5] S. C. Jacobsen et al., "Design of the UTAH/M.I.T. Dexterous Hand", *Proceedings 1986 IEEE International Conference on Robotics and Automation*, Vol. 3, pp. 1520-1532, 1986
- [6] C. S. Lovchik and M. A. Diftler, "The Robonaut Hand: A Dexterous Robot Hand For Space", *Proceedings of the 1999 IEEE International Conference on Robotics and Automation*, pp.
- [7] M. T. Mason and J. K. Salisbury, *Robot Hands and the Mechanics of Manipulation*, Cambridge, Massachusetts: The MIT Press, 1985.
- [8] P. J. McKerrow, *Introduction to Robotics*, Addison-Wesley Publishing Company, Inc, 1991.
- [9] A. M. Ramos, I. A. Gravagne and I. D. Walker, "Goldfinger: A Non-Anthropomorphic, Dexterous Robot Hand", *Proceedings of the 1999 IEEE International Conference on Robotics and Automation*, pp. 913-919
- [10] S. Schulz, C. Pylatiuk, G. Bretthauer, "A New Ultralight Anthropomorphic Hand", *Proceedings of the 2001 IEEE International Conference on Robotics and Automation*, pp. 2437-2441
- [11] G. A. Sohl and J. E. Bobrow, "Experiments and Simulations on the Nonlinear Control of a Hydraulic Servosystem," *IEEE Transactions on Control Systems Technology*, Vol. 7, pp. 238-247, March 1999
- [12] W. T. Townsend, "The BarrettHand grasper - programmably flexible part handling and assembly", *Industrial Robot: An International Journal*, Vol. 27, No. 3, 2000, pp. 181-188
- [13] J. Watton, *Fluid Power Systems: Modeling, Simulation, Analog and Microcomputer Control*, Hertfordshire, England: Prentice Hall International, 1989.